Aust. J. Phys., 1977, **30**, 187–207

Observations of Neutral Hydrogen in Bright Southern Galaxies

J. B. Whiteoak and F. F. Gardner

Division of Radiophysics, CSIRO, P.O. Box 76, Epping, N.S.W. 2121.

Abstract

Neutral hydrogen was detected in 36 out of 46 galaxies observed at 21 cm wavelength. Eighteen of the larger ones were partially mapped, and estimates of hydrogen and total mass obtained. Without correction for optical depth effects, median values of M_H and M_H/M_T were $7{\cdot}5 \times 10^9 M_\odot$ and 0·07 respectively. These values are similar to the average values found previously for Sc–Scd galaxies (the median morphological type for the sample). The lowest M_H/M_T ratios were found for NGC 253 and 4945, probably because of absorption of the nuclear continuum in addition to any hydrogen self-absorption.

Introduction

Although the neutral hydrogen content of many galaxies has been widely investigated, very few galaxies at high southern declinations have been included in the studies. At Parkes, previous observations have been limited to the most extended southern objects (van Damme 1966; Robinson and van Damme 1966; Shobbrook and Robinson 1967; Lewis 1969). To help overcome this lack of data, we have carried out a hydrogen-line survey of the brightest southern galaxies. In this paper we present the results for a total of 46 objects, 36 of which were found to contain detectable neutral hydrogen.

Equipment and Observations

The observations were obtained in July 1973 with the Parkes 64 m radio telescope. At 1420 MHz the beamwidth was 14′·8 arc. An uncooled 21 cm receiver, yielding an overall system temperature of about 120 K on cold sky, was employed in conjunction with a 1024-channel digital correlator operating in the total power mode. A combination of 512 channels and 10 MHz bandwidth (equivalent to an instantaneous velocity coverage of 2100 km s^{-1}) was generally used; this provided an effective resolution of 39 kHz (8·2 km s^{-1} in radial velocity) after Hanning smoothing.

The HI spectrum for each galaxy was generally derived from differencing two spectral observations each of 15 min duration, one with the telescope directed towards the galaxy and the other at a right ascension 17 min east of the galaxy. Because the two observations took place over the same range of telescope elevation, baseline effects which vary with elevation were removed. Intensity calibration of the spectra was effected using continuum observations of the radio sources associated with the galaxies NGC 253 (PKS 0045−25), 1068 (0240−00), 4696 (1245−41) and 4945 (1302−49). The flux dencities of the sources were taken from the Parkes catalogue of radio sources. Division of these flux densities by 1·6 yielded the antenna temperatures appropriate to the observations. The corresponding beam efficiency was 81%.

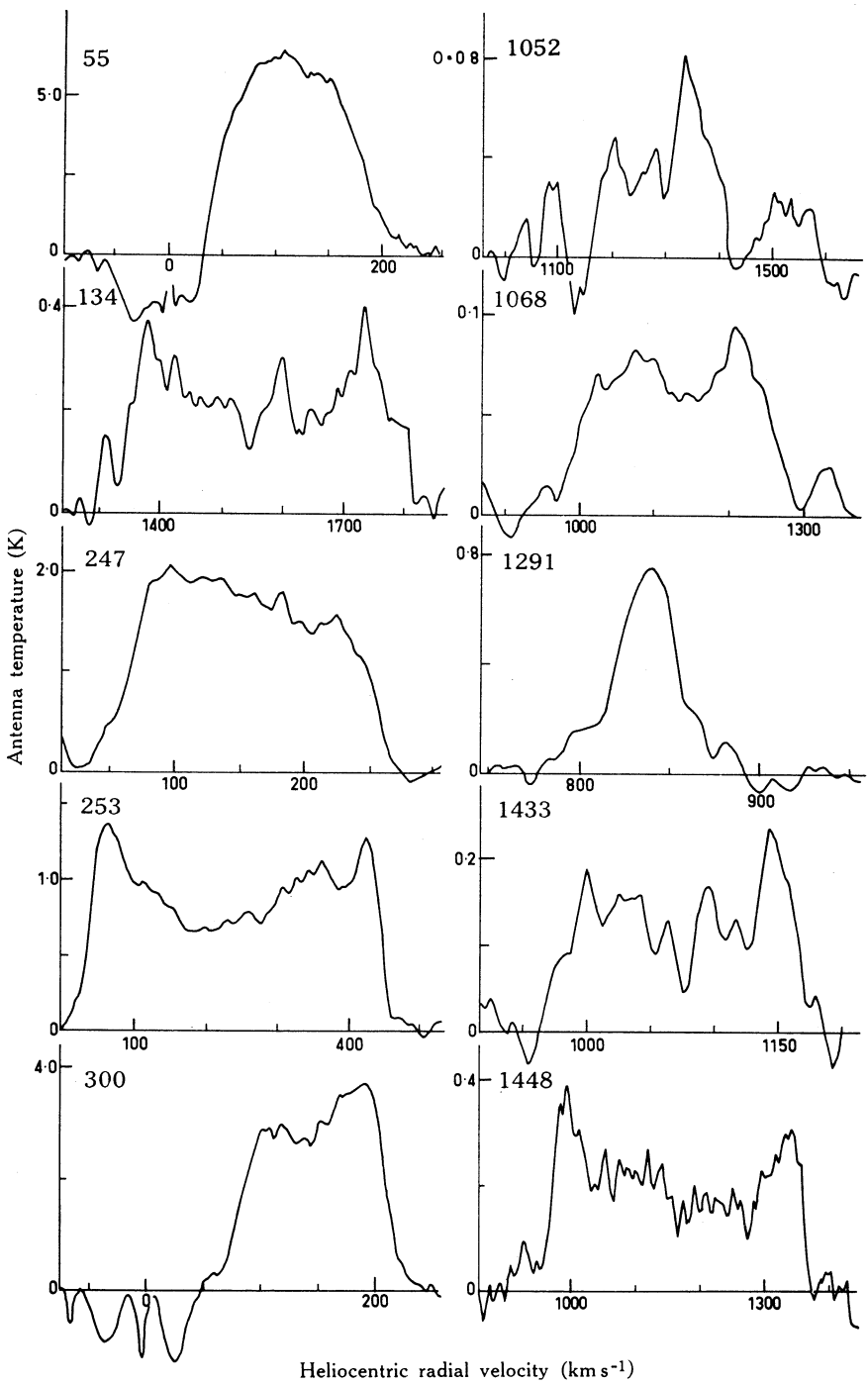

Fig. 1. HI profiles at the optical centres of the galaxies identified by their NGC numbers.

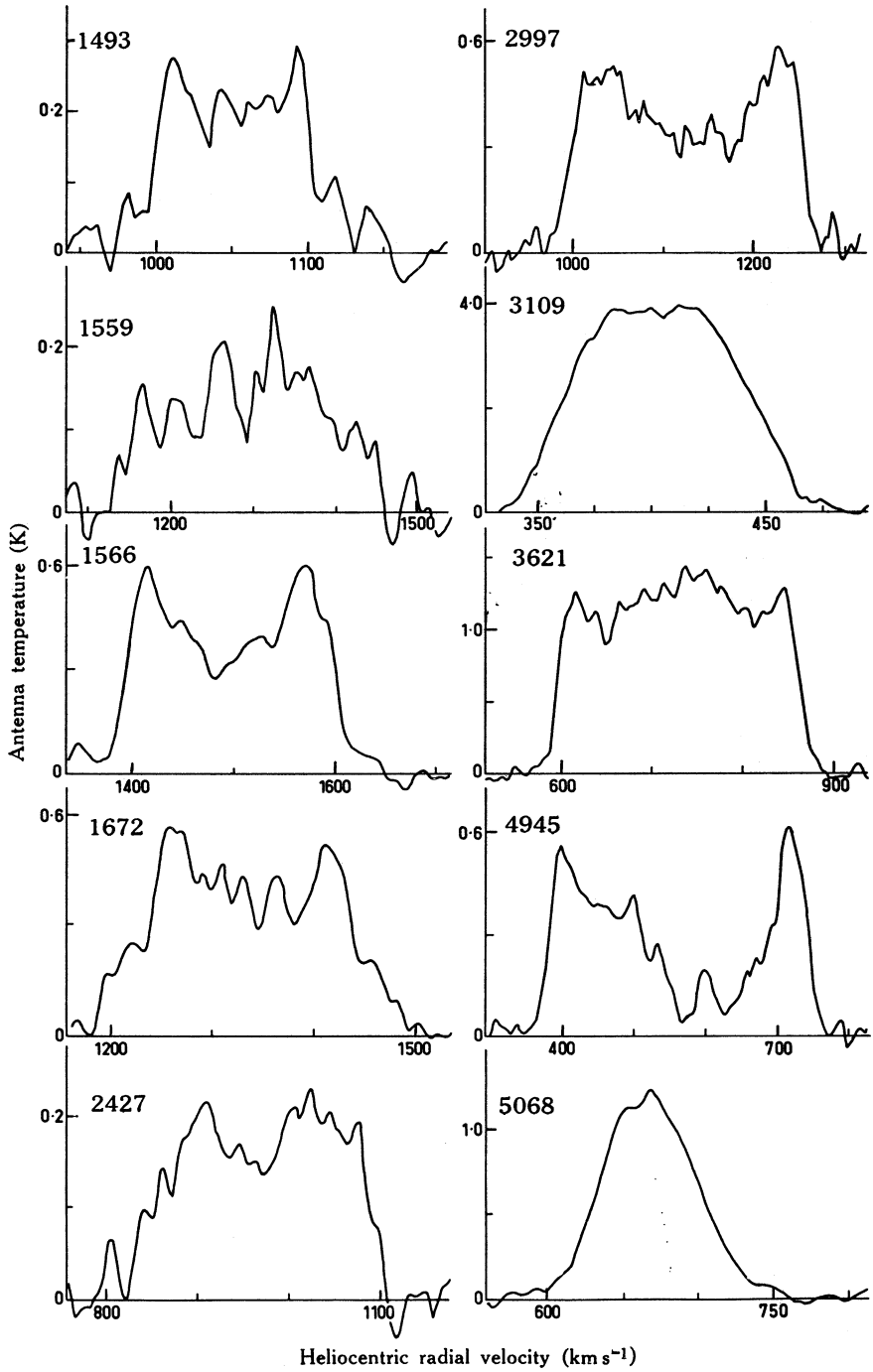

Fig. 2. HI profiles at the optical centres of the galaxies identified by their NGC numbers.

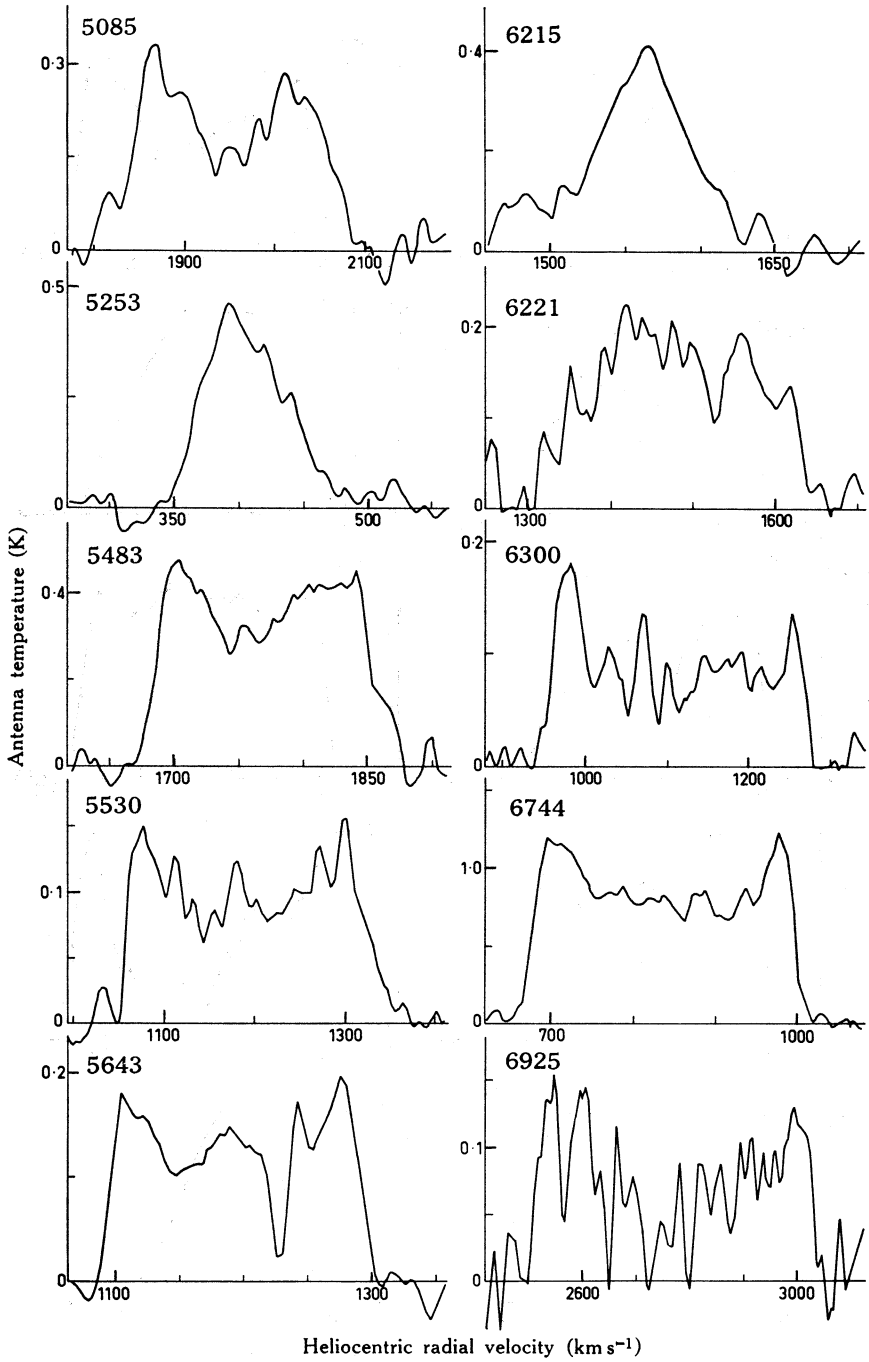

Fig. 3. HI profiles at the optical centres of the galaxies identified by their NGC numbers.

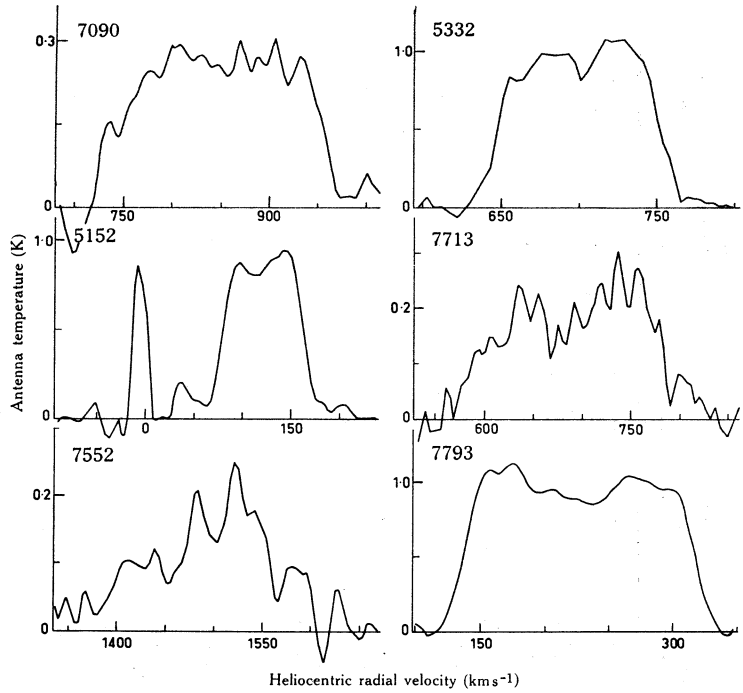

Fig. 4. HI profiles at the optical centres of the galaxies identified by their NGC or IC (5152 and 5332) numbers.

For a single pair of observations and 8 km s^{-1} resolution, the r.m.s. noise was about 0·035 K in antenna temperature. However, in cases where the peak antenna temperature of the HI profile was below 1 K, the noise in the final spectrum is lower because at least two sets of observations were made.

A total of 46 galaxies was selected from the Reference Catalogue of Bright Galaxies (de Vaucouleurs and de Vaucouleurs 1964) on the basis of one or other of the following criteria: optical magnitude, angular size, morphological type or optical radial velocity. In all cases, observations were made at the positions listed in this catalogue. For galaxies where the HI distribution extended over several minutes of arc, additional spectra were obtained at intervals of approximately 7′ along orthogonal axes (aligned with the optical major and minor axes where these are known). For a few large galaxies including NGC 253, 4945 and 6744, directions away from these axes were also sampled. The pointing accuracy for the observations was better than 1′.

Results

For the 36 galaxies in which HI emission was detected, the HI profiles at the optical positions are shown in Figs 1–4. The baselines beyond the extent of the HI emission have generally been curtailed. However, the zero levels were constructed on the basis of the total baseline. The low-velocity regions of profiles for galaxies such as NGC 55 and 300 are affected by HI in our Galaxy. The contribution from local hydrogen to each profile represents the difference between the spectra observed in the direction of the individual galaxy and at the reference position. For three large

Table 1. Details of observed galaxies

(1)	(2)	(3)	(4)	(5)	(6)	(7)	(8)	(9)	(10)	(11)
		Optical characteristics*			HI parameters (galaxy centre)					
Galaxy (NGC)	Type	Mag. B(0) or m_c	Dimensions (′ arc)	Rad. vel. V (km s^{-1})	T_A (K)	Syst. rad. vel. (km s^{-1})	Profile width (km s^{-1})	Profile area (K km s^{-1})	Distance D (Mpc)	Calc. mass M_{HI} ($10^9 M_\odot$)
55	SB(s)m	8·1	30×4·9	131	6·4	116	151	781±55	2·4	1·7
134	SAB(s)bc	11·2	7·2×2·0	1600	0·4	1566	493	114±11	31	41
247	SAB(s)d	9·9	21×7·4	−156	2·1	156	207	334±23	3·4	1·5
253	SAB(s)c	8·2	24×6·3	96	1·3	239	386	425±30	3·4	1·8
300	SA(s)d	9·9	20×14·1	145	3·7	146	142	412±29	2·4	0·9
625	SBm	12·6	2·9×1·2		<0·05	(781–2904)				
1052	E4	12·1	1·6×1·1	1460	0·07	1300	261	13±3	26	3·2
1068	(R)SA(rs)b	9·8	5·3×4·5	1050	0·08	1130	290	21±4	23	4·1
1291	(R)SB(s)0/a	10·2	5·8×3·9	802	0·8	836	58	32±5	14	2·2
1433	SB(r)a	10·9	6·0×5·0	974	0·2	1069	205	27±5	18	3·2
1448	SAcd	11·7	7·4×1·3		0·3	1161	406	81±10	20	11·7
1493	SB(r)cd	12·1	2·5×2·2		0·3	1051	132	27±5	17	3·0
1559	SB(s)cd	11·1	2·8×1·6		0·2	1291	306	41±6	21	7·0
1566	SAB(s)bc	10·1	7·2×5·8	1430	0·6	1497	222	96±10	26	24
1617	SB(s)a	11·4	3·6×1·7	788	<0·05	(325–2430)				
1672	SB(s)b	11·3	4·4×3·4	1300	0·6	1338	261	93±10	22	17·0
2427	SAB(s)dm	12·0	5·5×2·3		0·2	967	269	45±7	14	3·1
2997	SAB(rs)c	10·6	6·9×5·6		0·6	1084	271	112±11	16	10·8
3109	Im	10·6	14·1×3·1		3·9	404	108	342±23	2·2	0·6
3621	SA(s)d	10·2	11·2×7·6		1·4	731	275	320±22	9·4	11·3
4038/9	IBmP	11·2	7·1×4·3	1650	<0·05	(480–2603)				
4603	SA(s)c	12·2	3·5×2·2		<0·05	(484–2604)				
4696	E1	12·4	2·0×1·8	2733	<0·05	(1925–2988)				
4945	SB(s)cd	9·5	16·6×2·7		0·7	563	376	122±11	6·7	2·0
5068	SAB(rs)cd	11·1	6·3×5·8	570	1·2	669	97	90±9	10·2	3·5
5085	SA(s)c	12·1	3·2×2·8		0·3	1949	257	53±7	36	25
5253	IBmP	11·1	3·5×1·4	403	0·5	409	96	33±5	4·7	0·3
5483	SA(s)c	12·2	3·0×2·7		0·5	1773	187	66±8	32	25
5530	SAbc	12·1	3·6×1·9		0·1	1196	284	29±5	20	4·5
5643	SAB(rs)c	11·4	4·0×3·5	1145	0·2	1196	205	26±5	21	4·1

Table 1 (*Continued*)

(1)	(2)	(3)	(4)	(5)	(6)	(7)	(8)	(9)	(10)	(11)
		Optical characteristics*			HI parameters (galaxy centre)					
Galaxy (NGC)	Type	Mag. (B0) or m_c	Dimensions (′ arc)	Rad. vel. V (km s^{-1})	T_A (K)	Syst. rad. vel. (km s^{-1})	Profile width (km s^{-1})	Profile area (K km s^{-1})	Distance D (Mpc)	Calc. mass M_{HI} ($10^9 M_\odot$)
6215	SA(s)c	12·1	1·9 × 1·5	1510	0·4	1564	108	33 ± 5	29	10·1
6221	SB(s)c	11·8	3·0 × 2·1	1320	0·2	1482	315	49 ± 7	27	13·3
6300	SB(r)b	11·5	3·4 × 2·6		0·2	1110	321	30 ± 5	19	4·2
4721	SB(s)cd	12·7	3·8 × 1·3		< 0·05	(313–2432)				
6699	SAB(s)b	12·8	1·6 × 1·5	3420	< 0·07	(300–2500)				
6744	SAB(r)bc	9·8	14·5 × 9·1	790	1·2	835	332	289 ± 20	14	23
6753	(R)SA(r)b	12·1	2·2 × 1·9	3170	< 0·05	(126–3522)				
6810	SAa	12·6	2·9 × 0·8	2025	< 0·05	(763–2885)				
6907	SB(s)bc	12·2	2·7 × 2·4		< 0·10	(770–2890)				
6925	SA(s)bc	12·1	3·9 × 1·4	2619	0·1	2767	536	41 ± 6	57	47
7090	SBc	11·7	6·6 × 1·1	790	0·3	846	240	56 ± 7	16	5·2
5152†	IA(s)m	11·9	4·2 × 2·3	78	0·9	122	97	76 ± 8	(2)	(0·1)
7552	(R′)SB(s)ab	11·4	2·9 × 2·0	1600	0·2	1580	207	28 ± 5	31	10·2
5332†	SA(s)d	11·4	6·2 × 4·7		1·1	702	118	104 ± 10	14	7·7
7713	SBcd	11·9	4·0 × 1·7	667	0·2	686	219	39 ± 6	14	2·9
7793	SA(s)dm	10·4	8·3 × 5·8	200	1·1	227	193	177 ± 15	4·5	1·4

* Optical data from de Vauvouleurs and de Vaucouleurs (1964). † IC number.

Table 2. HI properties derived from galaxy mapping

(1)	(2)	(3)	(4)	(5)	(6)	(7)	(8)	(9)	(10)	(11)	(12)	(13)	(14)
							HI intensity peaks						
Galaxy (NGC)	Pos. angle °	Incl. i °	Profile offsets (′ arc)	HI dimensions (′ arc)	Mass corr. factor F	Corr. mass M_H ($10^9 M_\odot$)	Rad. vels (km s^{-1})	Sep. (′ arc)	Pos. angle °	Total mass M_T ($10^{11} M_\odot$)	$\frac{M_H}{M_T}$	Holmberg diam. (′ arc)	$\frac{M_i}{M_T}$
134	49*	77*	±7·7(49)	<4	1·0	41±4	1740,1381	7·0	(49)	⩾7·8	⩽0·053	8·7	0·78
247	172*	75*	±8·0(0,90),±16·0(0)	17×7	1·7	2·6±0·3	237,80	13·5	170	0·3±0·1	0·090	25·7	1·19
253	54*	79*	6·0 grid	16×11	2·1	3·8±0·4	60,427	14·5	54	1·1±0·2	0·035	28·5	1·32
1291		50	±7·0(0,90)	16×15	2·1	4·6±0·8							
1448	45	85	±7·1(45,135)	<4	1·0	11·7±1·1	1399,1060	5·5	45	2·5±0·5	0·038	8·0	0·91
1566	45	35	±6·0(0,90),±12·0(0)	8·5×8·5	1·3	31±4	1415,1570	6·8	47	3·7±0·6	0·083	10·7	0·98
1672	145	40	±7·0(0,90),±14·0(90)	7·5×<4	1·1	18·7±2·2	1262,1415	5·0	90	2·5±0·5	0·074	6·4	0·80
2997	93*	32*	±6·4,±12·9(0,90)	6×6	1·2	13·0±1·8	1189,993	6·9	101	4·0±0·6	0·032	10·2	0·92
3621	165	50	±7·0(0,90),±14·0(0)	16×8·5	1·7	19·2±2·3	613,845	16·3	170	2·8±0·5	0·069	15·7	0·60
4945	43	85	6·0 grid	19×4·5	2·1	4·2±0·5	718,404	13·9	48	1·9±0·3	0·023	17·6	0·79
5068		25	±7·0(0)	7·0	(1·2)	(4·2)							
5253	50	70	±6·9(60)	13	(1·15)	(0·3)							
5483	0	25	±7·1(0,90).±14·0(0)	14×8·5	1·6	40±6	1711,1823	6·6	172	5·8±0·9	0·069	4·5	0·43
6744	20	50	6·5 grid	20×15	2·4	55±6	982,695	17·0	12	6·2±0·7	0·088	20·5	0·75
7090	125	85	±7·0(50,140)	7·5×<4	1·1	5·7±0·9							
5332†	162*	36*	±7·1(0,90) ±14·1(90)	8·5×4·5	1·2	9·2±1·3	730,673	5·9	70	0·5±0·2	0·197	8·8	0·93
7713	170	65	±7·0(0,90)	8·5×8·5	1·15	3·3±0·6							
7793	105	45	±6·0,±12·0(0,90)	7·5×7·5	1·2	1·7±0·2	165,285	7·5	130	0·4±0·1	0·048	11·9	0·99

* Optical data from Danver (1942). † IC number.

galaxies that were previously investigated at Parkes (although with a lower velocity resolution of 30 km s^{-1}), namely, NGC 55 (Robinson and van Damme 1966), NGC 300 (Shobbrook and Robinson 1967) and NGC 3109 (van Damme 1966), the resolution was 4 km s^{-1} (compared with the value of 8 km s^{-1} that was used generally).

The galaxies observed, their optical parameters listed by de Vaucouleurs and de Vaucouleurs (1964), and the HI results are listed in Table 1. Several of the listed optical velocities (column 5) were obtained from the recent results of Martin (1976). The parameters describing the HI profiles (columns 6–9) consist of the peak antenna temperature T_A, the systemic heliocentric radial velocity, the profile width at the quarter-power level (this quantity has been previously used as a width parameter by Lewis and Davies (1973) and others), and the profile area A. The errors associated with A are standard deviations and include calibration and baseline errors. For galaxies in which no HI was detected, the maximum antenna temperature is listed together with the observed velocity range in parentheses. Most distances D (column 10) were derived from the systemic velocities after conversion to velocities relative to the centroid of the Local System (as described by de Vaucouleurs and de Vaucouleurs). A Hubble constant of 50 km s^{-1} Mpc^{-1} was adopted, as advocated by Sandage and Tammann (1975). For the nearest galaxies NGC 55, 247, 253, 300 and 3109, the distances listed are those given by either Roberts (1969) or Huchtmeier (1972). The last column of the table (column 11) lists the mass of neutral hydrogen M_{HI}, calculated from the expression

$$M_{HI}/M_{\odot} = 3{\cdot}76 \times 10^5 D^2 A,$$

where D is in Mpc and A is in K km s^{-1}.

Table 2 lists galaxies for which additional spectra were obtained at positions displaced from the optical nucleus. For the most extended cases, Figs 5–7 show the sequence of HI profiles along one axis (the approximate major axis, if known). Columns 2 and 3 of Table 2 show the position angle of the major axis and the inclination i of the plane of the galaxy to the plane of the sky, both quantities being obtained from optical parameters. Several of these parameters (indicated by asterisk) are from Danver (1942). Where Danver's values were not available, position angles were estimated by visual inspection of Palomar Sky Survey prints or the ESO(B) survey prints. In addition, the inclinations were calculated from the dimensions listed in Table 1, the values above 80° being further increased by up to 5° to allow for the finite thickness of the galaxies. In general, inclinations calculated in this manner are in reasonable agreement with Danver's values and with values calculated by the more elaborate method of Heidmann *et al.* (1972).

Column 4 of Table 2 contains the positional offsets from the centre at which additional spectra were observed. The numbers in parentheses designate the position angles (in degrees) of the offsets relative to the galaxy centre.

Most of the remaining columns contain information related to the observed HI distributions. The HI dimensions (column 5) are the half-intensity widths (after correction for the telescope beamwidth of 14′·8 arc) of gaussian distributions fitted to distributions of the profile areas along each of the orthogonal axes through the centre of the galaxy. If the uncorrected half-widths were not significantly greater than 14′·8, upper limits of 4′ are shown. In no case does the HI extent greatly exceed the telescope beamwidth, so that the total HI mass can be obtained by applying a

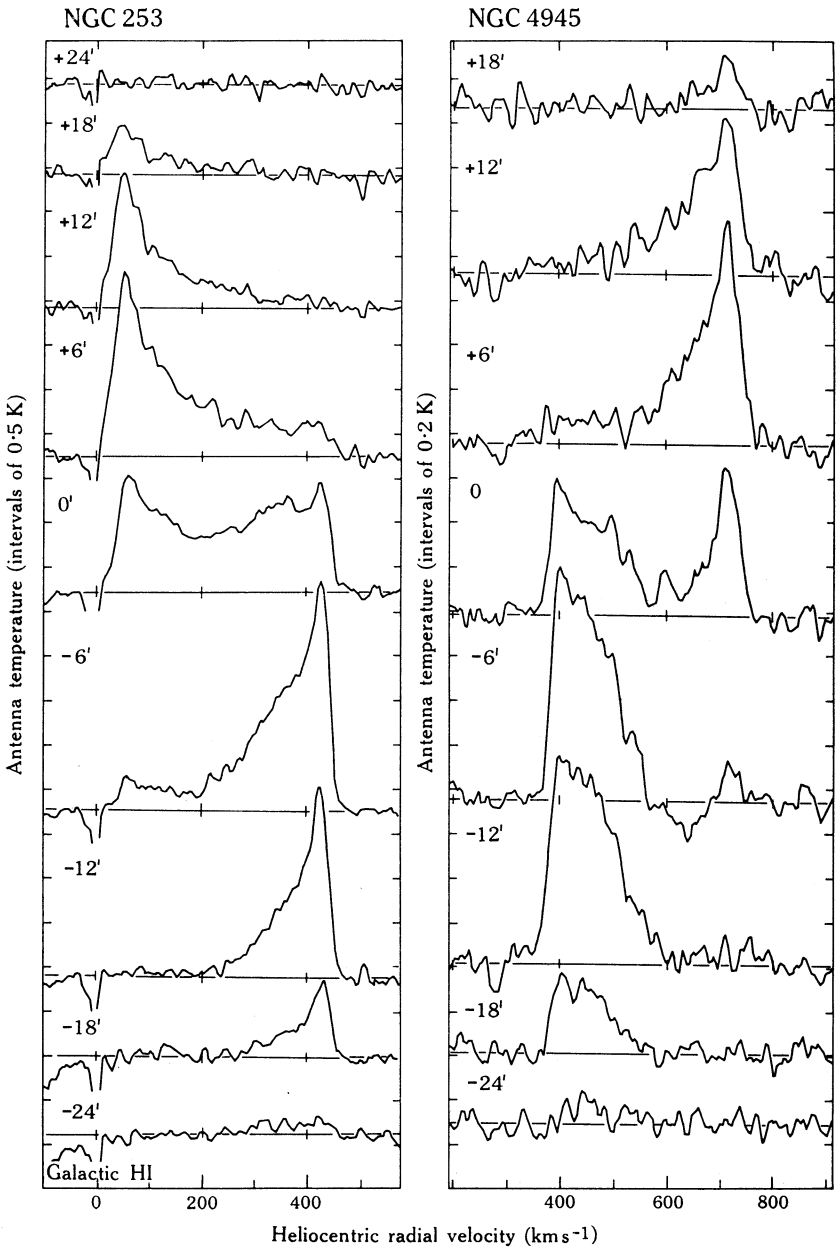

Fig. 5. HI profiles obtained at a series of offsets (as indicated in the figures) along the approximate major axis for NGC 253 and 4945. Positive values are to the north-east.

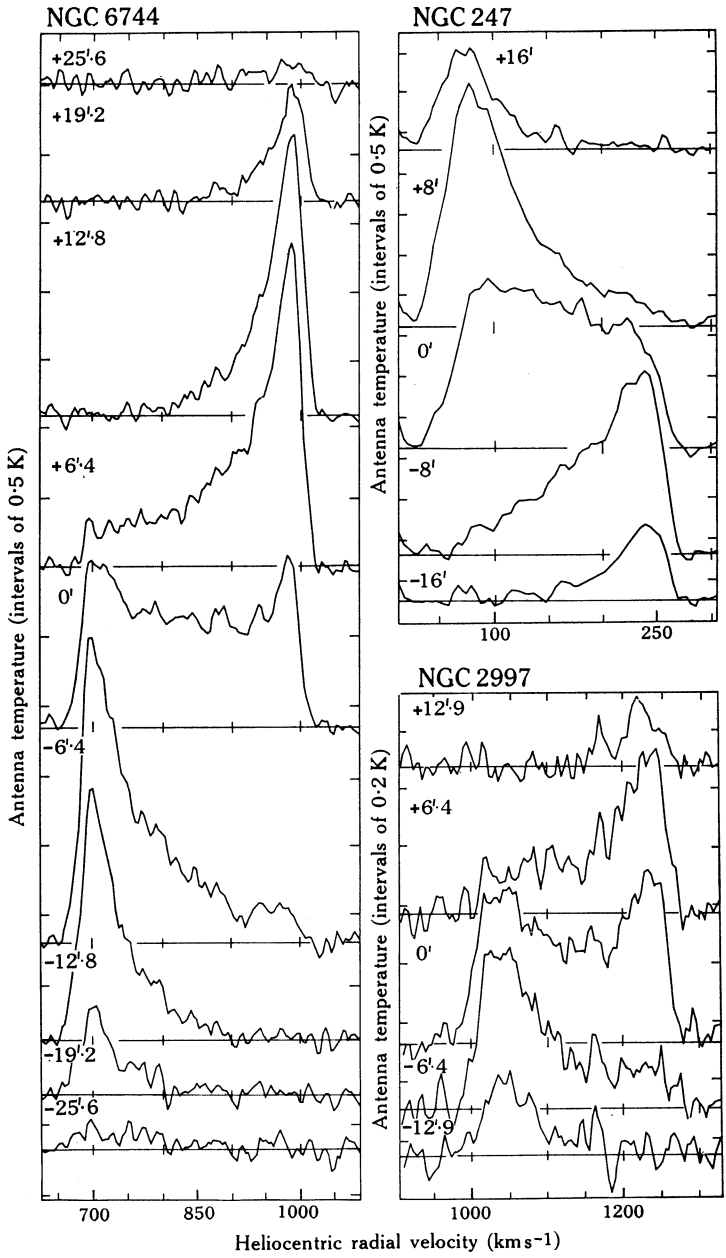

Fig. 6. HI profiles obtained at a series of offsets (as indicated in the figures) along the approximate major axis for NGC 6744, 247 and 2997. Positive offsets occur in the directions of the position angles listed in Table 2.

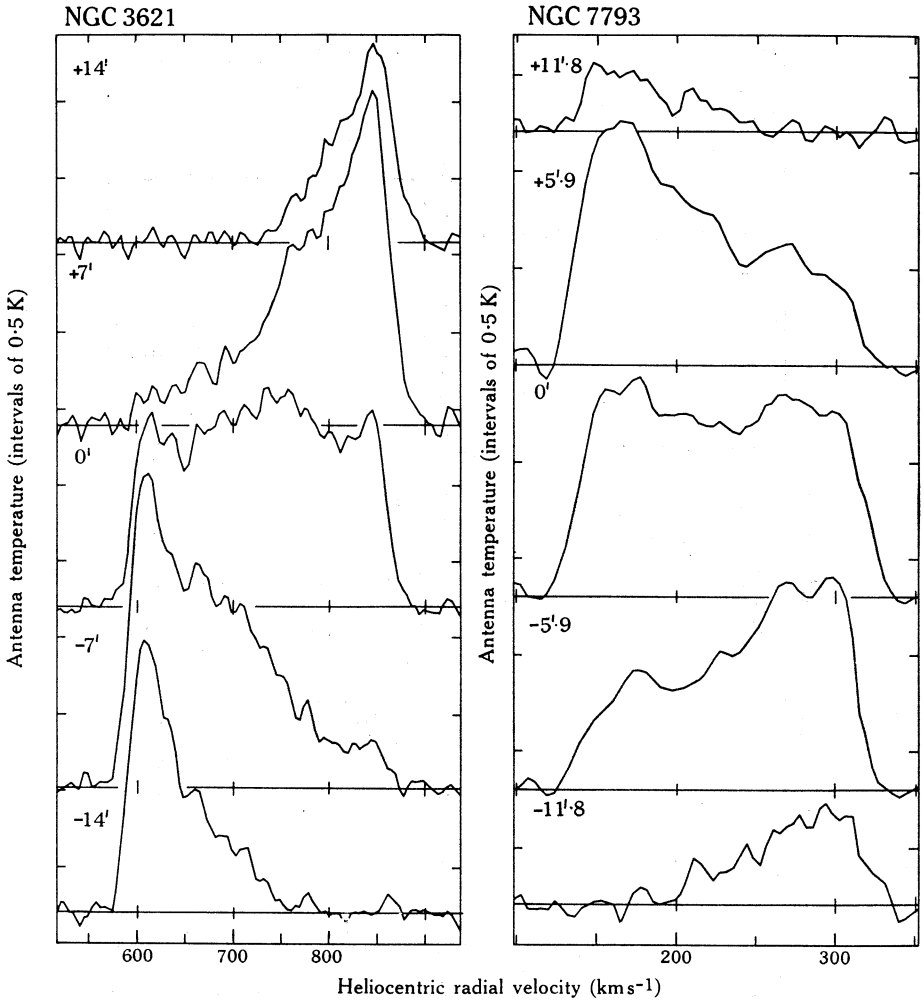

Fig. 7. HI profiles obtained at a series of offsets in declination for NGC 3621 and in right ascension for NGC 7793.

correction factor to the mass derived from the profile at the galaxy centre. In most cases, the mass correction factor F (column 6) is given by the product of the uncorrected HI dimensions divided by $(14 \cdot 8)^2$. For the extensively mapped galaxies NGC 253, 4945 and 6744, F was determined using the procedure outlined by Shobbrook and Robinson (1967). By means of the factors F, the corrected HI masses M_{H} (column 7) were calculated. The accompanying errors do not include errors in the Hubble constant.

The profiles for each galaxy generally indicate that the HI distribution peaks at two positions more or less equally displaced to each side of the galaxy centre along the major axis. Columns 8–10 of the table list the radial velocities the angular separation, and the position angle of separation of these peaks. For most galaxies this position angle represents the direction of intersection of the plane of rotation with the plane of the sky, and is therefore normal to the axis of rotation. The sense of

the velocity variation across the galaxy is such that the position angle shows the orientation of the peak at the first listed velocity relative to that at the second velocity. For NGC 134, where the HI profiles were observed along only one axis, the position angle is shown in parentheses, and it merely represents the direction in which the listed parameters were obtained.

Columns 11 and 12 show the total mass M_T and the ratio of hydrogen mass to total mass M_H/M_T. The total mass was estimated from the galaxy rotation shown in the HI results using the $n = 3$ form of the rotation curves discussed by Brandt (1960). This form is often used in general discussions (Roberts 1969; Shostak 1975), although there is evidence that individual galaxies may have rotation curves with n ranging between 1 and 5 (Rogstad and Shostak 1972; Huchtmeier 1975). For $n = 1$, 3 and 5, the calculated mass varies in the ratio $2{\cdot}2 : 1 : 0{\cdot}85$. For $n = 3$, the mass of a spiral galaxy is given by $M_T/M_\odot = 1{\cdot}12 \times 10^5 D V_m^2 \theta_m \operatorname{cosec}^2 i$ (see e.g. Rogstad *et al.* 1967), where D is in Mpc, while V_m is the maximum radial velocity relative to the systemic velocity (in $\mathrm{km\,s^{-1}}$) which is attained at an angular radius of θ_m minutes of arc along the major axis. For galaxy models that produce line profiles containing outer peaks, the results of Rogstad *et al.* suggest that θ_m is approximately half the separation of the intensity peaks. Assuming an exact equality and that V_m is half the quarter-power width of the profile, the above equation was used to calculate the entries in the table. For galaxies with low inclinations, the values of mass may be considerably in error due to the uncertainties in i. Because such errors are difficult to assess, they have not been included in the errors in the table. Column 13 gives the equivalent Holmberg diameter derived from the optical diameter in Table 1 in the way described by Heidmann *et al.* (1972). For galaxies for which no rotational data are available, Heidmann (1969) has proposed the use of the 'indicative total mass' M_i, which is derived from the profile width and the Holmberg diameter. The ratios M_i/M_T are listed in column 14.

HI Results for Individual Galaxies

NGC 55, 300 and 3109. These nearby large galaxies have been extensively studied elsewhere, and no mapping was undertaken in the present investigation. However, the profiles in the directions of the centres of these galaxies contain significantly more structure than in the previous studies with lower velocity resolution, suggesting that further mapping with the present resolution could be worth while.

NGC 134. Bottinelli *et al.* (1968) failed to detect HI emission in this galaxy.

NGC 247. As suggested in the central profile, the HI distribution is not symmetrical—the greater proportion of gas is located in the northern half of the galaxy. Profiles at offsets from the centre along the major axis are shown in Fig. 6.

NGC 253. Because the galaxy is quite extended, spectra were obtained for a grid of 35 positions separated by $6'{\cdot}0$ arc in directions either parallel or normal to an axis at position angle 52° (the approximate orientation of the major axis). At each of the velocities of the two intensity maxima in the profiles (60 and 427 $\mathrm{km\,s^{-1}}$), the HI emission has a gaussian distribution of observed halfwidths $17'$ and $15'$ in the direction of the major and minor axes.

The profiles at offsets from the centre along the major axis are shown in Fig. 5. Intensity isophotes derived from these profiles are shown on a velocity offset plot

in Fig. 8. There is a well-defined intensity ridge extending between the outer peaks. The locus of this ridge does not have the form of the rotation curves discussed by Brandt (1960)—near the peaks the ridge becomes parallel to the velocity axis, i.e. normal to the rotation curves. However, the behaviour is consistent with the models of Rogstad *et al.* (1967), which were based on these curves but which took into account the effect of rotation on the centroid of the HI distribution observed at each radial velocity. Because of this interaction and the finite beamwidth, each centroid has a major axis offset greater than the value appropriate to the true rotation curve. The displacement of the peaks in the figure are consistent with the HI study of the galaxy made by Huchtmeier (1972) with higher angular resolution along the major axis (about 5′ arc).

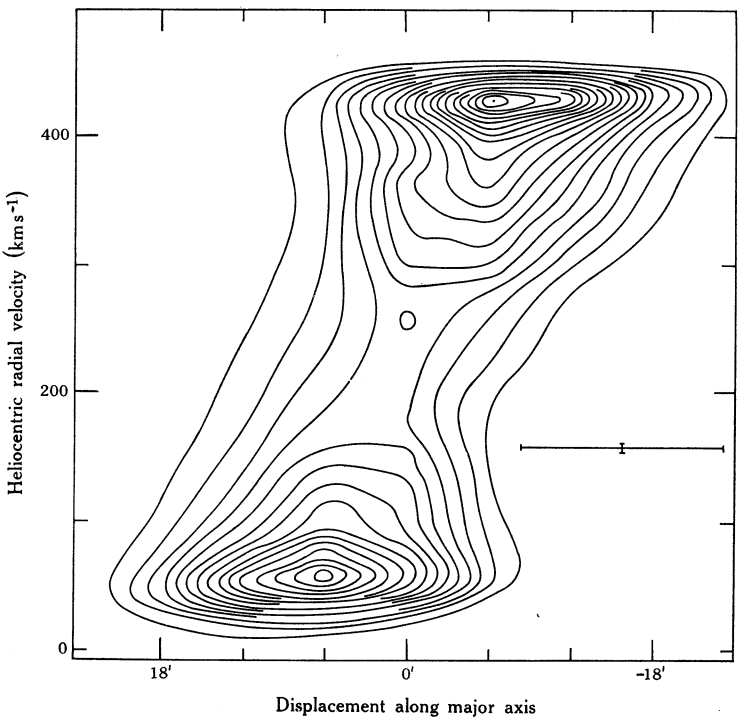

Fig. 8. Intensity isophotes for NGC 253 on a velocity–offset plot. The contour interval is 0·125 K antenna temperature. Resolution in velocity and angle is indicated.

The galaxy is of particular interest because of the detection of OH and H_2CO absorption against the small-diameter radio source associated with the nucleus (Whiteoak and Gardner 1973; Gardner and Whiteoak 1974). More recently, Gottesman *et al.* (1976), using an interferometer to resolve out the extended HI emission, have detected HI absorption at velocities between 100 and 300 km s^{-1}. The presence of this absorption probably causes the asymmetry in the region between the outer peaks of the HI profile obtained in the direction of the nucleus.

Huchtmeier (1972) has estimated that the south-west side of the galaxy contains 30% more HI than the north-east side. This is not supported by the present study, in which the ratio of (hydrogen mass SW.) to (hydrogen mass NE.) is 0·98. It is

unlikely that the larger east–west beamwidth of the Parkes telescope could have removed the asymmetry.

One interesting feature in the profiles, which is common to the results for several other galaxies, is the narrowness of the two outer intensity peaks. The narrow half-width (typically around 50 km s^{-1}) and prominence of the peaks both point to the existence of a narrow ring or spiral feature containing HI, as suggested by Huchtmeier (1972).

NGC 1291. The narrow profile is typical of a galaxy virtually face-on to the line of sight. However, the additional spectra suggest that there is an axis of rotation near position angle 135°, with the HI at the higher velocities concentrated more to the north-east. This differs from the almost north–south elongation of the inner optical regions of the galaxy as shown in the Whiteoak extension of the Palomar Survey, but is consistent with the slight elongation of an optically diffuse outer ring. The velocity gradient is small—for a change of 17 km s^{-1} near the systemic velocity the HI centroid changes 6′·4 arc.

The HI dimensions (16′ × 15′ arc) greatly exceed the listed optical dimensions (5′·8 × 3′·9 arc). However, de Vaucouleurs (1956) has noted optical extensions with a diameter of 30′. The HI content of this galaxy is anomalous (this has been discussed by Lewis 1970). Although the galaxy has a Hubble type of S0, its hydrogen mass $4{\cdot}6 \times 10^9 M_\odot$ is more appropriate to a spiral galaxy (see Balkowski 1973).

NGC 1672. The central profile is unusual in that, in addition to the two main peaks, there are outer shoulders with velocities near 1214 and 1460 km s^{-1}. This suggests the existence of an outer ring of HI displaced 6′ to 7′ arc from the galaxy centre (compared with 2′·5 for the main peaks).

NGC 2997. Fig. 6 shows the HI profiles obtained at intervals of 6′·4 arc in right ascension. This direction is similar to the optical major axis 93° (position angle), and almost normal to the axis of rotation (11°), as implied by the HI data listed in columns 8–10 of Table 2.

NGC 3621. Fig. 7 shows the HI profiles at intervals of 7′·0 arc in declination. This direction is close to the optical major axis (position angle 165°) and also normal to the axis of rotation (80°).

NGC 4945. The HI distribution in this bright edge-on spiral galaxy is very extended, and profiles were obtained for a grid of 32 positions separated by intervals of 6′·0 arc in directions parallel and normal to an axis at position angle 41° (i.e. approximately parallel to the optical major axis). The profiles along the major axis are shown in Fig. 5. HI is observable even at offsets of ±24′ from the galaxy centre. In contrast to results found for other edge-on spiral galaxies, there appears to be a lack of HI emission towards the centre of the galaxy.

There are several reasons for believing that the HI deficiency is caused by HI absorption against the nuclear radio source in this galaxy. These reasons have been discussed in detail by Whiteoak and Gardner (1976). Firstly, the negative HI temperature near 650 km s^{-1} at an offset of −6′ arc in Fig. 5 can only be explained in terms of absorption. This feature can be seen more clearly in Fig. 9, which shows the spatial distribution of line temperature at velocities between 630 and 650 km s^{-1}. The negative feature is well defined, with a maximum absorption temperature of about 0·15 K.

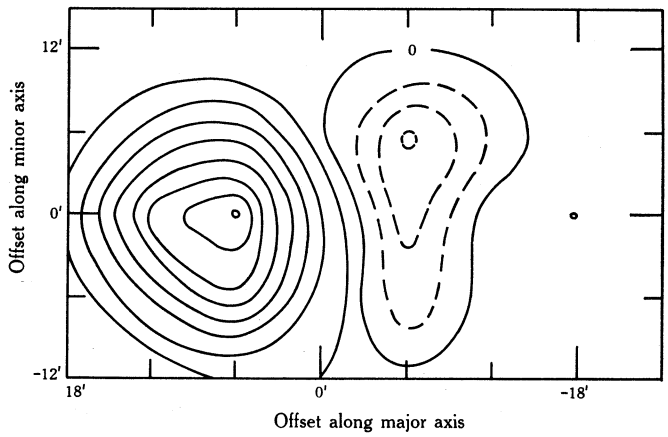

Fig. 9. Spatial distribution of HI line temperature at velocities between 630 and 650 km s^{-1} for NGC 4945. Contour intervals are 0·05 K antenna temperature. Negative contours are shown as dashed lines.

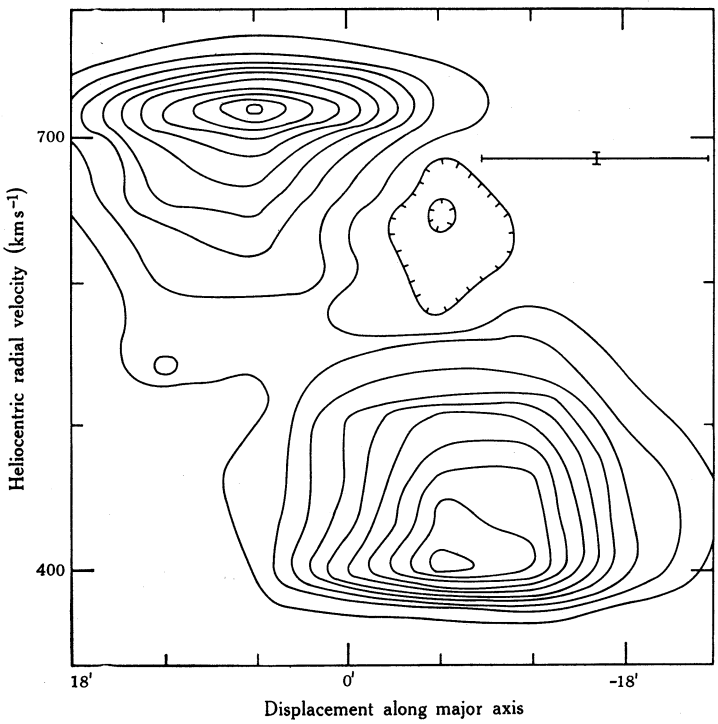

Fig. 10. Intensity isophotes for NGC 4945 on a velocity–longitude plot. The contour interval is 0·1 K antenna temperature, and negative contours are shown ticked. Resolution in velocity and angle is indicated.

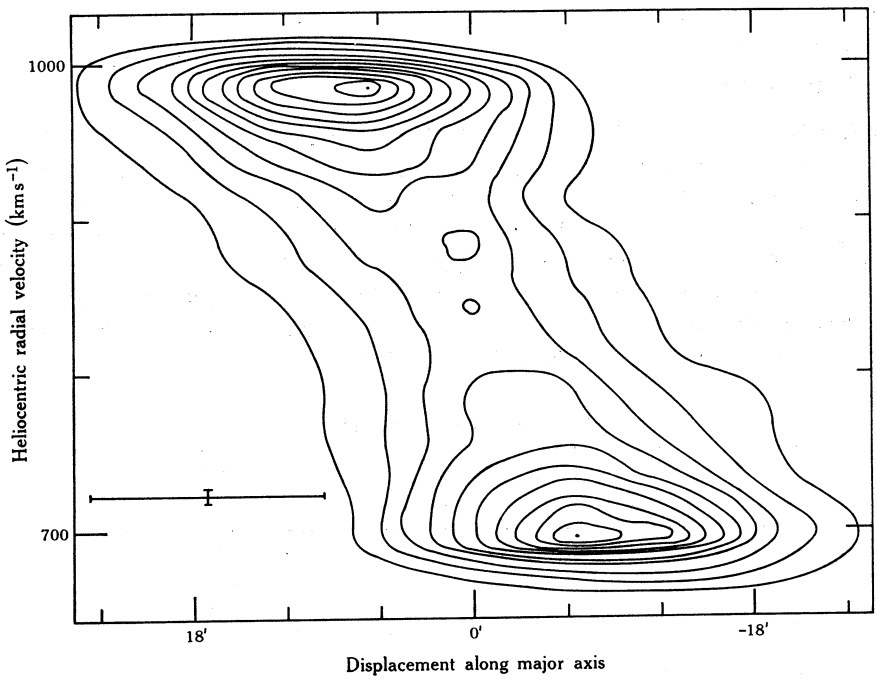

Fig. 11. Intensity isophotes for NGC 6744 on a velocity–offset plot. The contour interval is 0·2 K antenna temperature. Resolution in velocity and angle is indicated.

The displacement of the peak absorption from the galaxy centre is spurious, a consequence of beam smoothing of an HI distribution consisting of: (*a*) an HI emission distribution displaced to positive major-axis offsets by the effect of rotation of the galaxy; (*b*) HI absorption of 0·3 K against the nuclear radio source of angular size only 30″ arc (Shobbrook and Shaver 1967).

Further evidence for absorption is the similarity between the shape of the inner parts of the HI profile obtained at the galaxy nucleus and the shapes of the OH and H_2CO absorption-line profiles observed in the same direction (see Fig. 1 of Gardner and Whiteoak 1974). From such a comparison, Whiteoak and Gardner (1976) deduced a maximum HI absorption temperature of 0·4 K, which corresponded to an optical depth of about 0·16.

Intensity isophotes derived from the profiles in Fig. 5 are shown on a velocity–longitude plot in Fig. 10. In contrast to the results for NGC 253 (Fig. 8), there is no well-defined ridge between the two outer intensity peaks. This is no doubt another manifestation of the presence of an absorption component in the HI profiles.

NGC 5068. This is another case showing a single narrow HI profile typical of an almost face-on galaxy. The profiles at the offset positions (in declination) are similar in shape but differ slightly in velocity, presumably owing to rotation. The centroids of the HI distributions at velocities displaced by ± 12 km s^{-1} from the systemic velocity are separated by 2′·3 arc (with velocity increasing to the north).

NGC 5253. This irregular galaxy appears on the Palomar Sky Survey prints to be inclined to the line of sight, with a major axis near 50°. However, the HI profile is

single peaked, and the profiles obtained at the offset positions provide no evidence for rotation. The HI halfwidth of 13′ arc is considerably larger than the quoted optical dimensions (3′·5 × 1′·4 arc).

NGC 6744. Because of the extended HI distribution this galaxy was observed over a grid of 31 positions separated on average by intervals of 6′·5 arc in directions parallel and normal to an axis through the galaxy centre at a position angle of 20° (the approximate major axis). The profiles obtained along the major axis are shown in Fig. 6. As for the extended distribution discussed earlier, the outer intensity peaks become most prominent in the offset profiles. The intensity isophotes derived from these profiles are shown on a velocity–longitude plot in Fig. 11. The characteristics of the plot are similar to those for NGC 253.

Table 3. Comparison of M_H and M_T values

NGC	D (Mpc)	M_H ($10^9 M_\odot$)	M_T ($10^{11} M_\odot$)	Reference
247	3·4	7·2	0·8	Lewis (1969)
		3·2	0·3	Roberts (1969)
		1·8	0·3	Balkowski (1973)
		2·6	0·3	Present results
253	3·4	7·8	2·6	Lewis (1969)
		7·4	1·7	Roberts (1969)
		7·8	1·3	Huchtmeier (1972)
		3·4		Balkowski (1973)
		3·8	1·1	Present results
1068	23	5·5	4·4	Allen *et al.* (1971)
		11·3		Lewis and Davies (1973)
		4·1		Present results
1291	14	19·0		Lewis (1970)
		4·6		Present results
2997	16	14·0	5·0	Balkowski (1973)
		13·0	4·0	Present results
3621	9·4	15·8		Gouguenheim (1969)
		14·7	2·3	Balkowski (1973)
		19·2	2·8	Present results
5253	4·7	0·2		Bottinelli *et al.* (1972)
		0·3		Lewis and Davies (1973)
		(0·3)		Present results
7793	4·5	1·2		Gouguenheim (1969)
		1·3		Roberts (1969)
		1·2	0·3	Balkowski (1973)
		1·7	0·4	Present results

NGC 7090. The profiles are rather weak and show no well-defined evidence of rotation. If anything, the centroid of the profile may be at a higher velocity in the south-east direction than in the north-west.

IC 5332. The results are anomalous in that the optical major axis (position angle 162°) is almost parallel to the deduced axis of rotation (160°).

NGC 7713. Within the limits imposed by low intensities, the profile shapes varied little with position. The HI at higher velocities may be more concentrated east of the galaxy centre.

NGC 7793. Fig. 7 shows the HI profiles obtained along an east–west axis (which is close to the major axis position angle of 105°). The results indicate that the axis of rotation is not normal to the major axis of the galaxy.

Discussion

Comparison with Previous Results

In Table 3, a comparison is made between the values of M_H and M_T listed in Table 2 and the corresponding values determined for the same galaxies in other surveys. All the values have been scaled to the distances listed in Table 1 according to the equations given in the previous section. The largest disagreements in M_H occur for the edge-on galaxies NGC 247 and 253. Apart from the high value given for NGC 253 by Huchtmeier (1972), the differences are due to the scaling corrections applied for the increased optical depth at high inclinations. For instance, Lewis (1969) used a factor of about 3, Roberts (1969) a value approaching 2 and Balkowski (1973) a value of 1·1, while the present results are uncorrected. When these factors are removed the agreement is more satisfactory. There is evidence in Table 2 supporting an increase of optical depth with inclination: the median values of M_H and M_H/M_T for galaxies with inclinations above 70° are about half of those for galaxies with lower inclinations. However, the sample of galaxies is not sufficiently large to yield accurate scaling factors and, because of the obvious disagreement in the correction factors adopted by other observers, no corrections were applied in the tables.

There is another discrepancy in the listed M_H values for NGC 1291. It arises because Lewis (1970) used the mean parameters of early-type galaxies to scale up by a factor of seven the mass obtained from the central profile. A decrease of this factor to two, a value similar to that used in Table 2, would yield a value of $5 \cdot 7 \times 10^9 M_\odot$ for M_H and remove the discrepancy.

For the five cases where the present values of M_T can be compared with previous estimates there is no significant evidence of any systematic differences. If anything, the estimates of Lewis (1969) appear higher than those of other observers.

Overall Statistics

Although it would be unwise to generalize too much (because the observed sample was composed mainly of galaxies most likely to contain detectable HI emission) some tentative conclusions may be drawn from the results given in Table 2.

For the 18 galaxies listed in Table 2 the median morphological type is Sc–Scd on the Hubble system, and type 5–6 in the system used by de Vaucouleurs and de Vaucouleurs (1964). The median ratio of the HI halfwidth to the Holmberg diameter is 0·7. This suggests that, if the HI has a gaussian distribution, there is a significant amount of gas beyond the optical limits.

The median ratio of the angular separation of the HI peaks to the Holmberg diameter is also 0·7. Huchtmeier (1975) has deduced that the ratio of 'turnover' radius to Holmberg radius for a galaxy of type Sc–Scd is about 0·8. The similarity of the values of the two ratios lends support to our earlier assumption that the turnover radius is approximately equal to half the angular separation of the HI peaks.

The median ratio of M_i/M_T is 0·9, which suggests that on average the indicative mass, derived from the optical Holmberg diameter, has a value similar to the mass derived entirely from the HI observations; both are based upon a rotation curve of the $n = 3$ form.

The median value of M_H is $7{\cdot}5 \times 10^9 M_\odot$. It is similar to the corresponding values (6×10^9–$5{\cdot}5\times10^9$) for Sc–Scd galaxies in the more comprehensive lists of Balkowski (1973) and Shostak (1975), after scaling all distances to a Hubble constant of 50 $\mathrm{km\,s^{-1}\,Mpc^{-1}}$. However, these values are significantly lower than that (16×10^9) derived by Roberts (1974). The difference probably reflects the large corrections that Roberts used to allow for increasing HI optical depth with inclination—small or no corrections were used in the other studies (e.g. Shostak was unable to detect any effect of inclination on optical depth).

Our median value for M_H/M_T is 0·07. It lies between the value 0·04 derived by Balkowski (1973) using indicative mass, and the values of 0·15 and 0·13 for the galaxies listed by Roberts (1974) and Shostak (1975). Roberts's high ratio is a consequence of his high M_H estimates mentioned previously. Shostak's value is higher than ours probably because he adopted a turnover radius equal to 1/6 of the Holmberg diameter for his calculations of M_T. In contrast, for our median galaxy, the parameter that we used as turnover radius (half the angular separation of the HI peaks) is 0·35 times the Holmberg diameter. Because the same form of rotation curve was used in both calculations, our values of M_T are therefore on average twice as large as those of Shostak.

Conclusions

For galaxies inclined significantly to the line of sight, the line profile for the total HI in the galaxy extends over several hundred $\mathrm{km\,s^{-1}}$ (an effect of rotation), and shows characteristic outer intensity peaks. Although some of the peaking may be a consequence of the velocity turnover shown in the rotation curve, the narrowness of the peaks for some galaxies could only be caused by an annular concentration of HI. In general, the axis of rotation is almost perpendicular to the direction of elongation shown by the optical distribution, although there is one exception, IC 5332, where the two directions are almost parallel.

The median hydrogen mass of $7{\cdot}5 \times 10^9 M_\odot$ is similar to values obtained in other surveys of Sc–Scd galaxies before correction for optical depth effects. The ratio M_H/M_T of 0·07, derived solely from HI data (in contrast with estimates from other surveys) is within the spread of values obtained elsewhere. As mentioned above, we made no attempt in this survey to observe a homogeneous sample of galaxies. Conclusions with higher statistical significance should result from the completion of a comprehensive survey now being undertaken with the Parkes telescope by other observers.

References

Allen, R. J., Darehy, B. F., and Lauqué, R. (1971). *Astron. Astrophys.* **10**, 198.
Balkowski, C. (1973). *Astron. Astrophys.* **29**, 43.
Bottinelli, L., Gouguenheim, L., and Heidmann, J. (1972). *Astron. Astrophys.* **17**, 445.
Bottinelli, L., Gouguenheim, L., Heidmann, J., and Heidmann, N. (1968). *Ann. Astrophys.* **31**, 205.
Brandt, J. C. (1960). *Astrophys. J.* **131**, 293.
van Damme, K. J. (1966). *Aust. J. Phys.* **19**, 687.

Danver, C. (1942). *Ann. Lund Obs.* No. 10.
Gardner, F. F., and Whiteoak, J. B. (1974). *Nature* **247**, 526.
Gottesman, S. T., Lucas, R., Weliachew, L., and Wright, M. C. H. (1976). *Astrophys. J.* **204**, 699.
Gouguenheim, L. (1969). *Astron. Astrophys.* **3**, 281.
Heidmann, N. (1969). *Astrophys. Lett.* **3**, 153.
Heidmann, J., Heidmann, N., and de Vaucouleurs, G. (1972). *Mem. R. Astron. Soc.* **75**, 85.
Huchtmeier, W. (1972). *Astron. Astrophys.* **17**, 207.
Huchtmeier, W. (1975). *Astron. Astrophys.* **45**, 259.
Lewis, B. M. (1969). Ph.D. Thesis, Australian National University.
Lewis, B. M. (1970). *Observatory* **90**, 264.
Lewis, B. M., and Davies, R. D. (1973). *Mon. Not. R. Astron. Soc.* **165**, 213.
Martin, W. L. (1976). *Mon. Not. R. Astron. Soc.* **75**, 633.
Roberts, M. S. (1969). *Astron. J.* **74**, 859.
Roberts, M. S. (1974). *Science* **183**, 371.
Robinson, B. J., and van Damme, K. J. (1966). *Aust. J. Phys.* **19**, 111.
Rogstad, D. H., Rougoor, G. W., and Whiteoak, J. B. (1967). *Astrophys. J.* **150**, 9.
Rogstad, D. H., and Shostak, G. S. (1972). *Astrophys. J.* **176**, 315.
Sandage, A., and Tammann, G. A. (1975). *Astrophys. J.* **196**, 313.
Shobbrook, R. R., and Robinson, B. J. (1967). *Aust. J. Phys.* **20**, 131.
Shobbrook, R. R., and Shaver, P. A. (1967). *Observatory* **87**, 169.
Shostak, G. S. (1975). *Astrophys. J.* **198**, 527.
de Vaucouleurs, G. (1956). *Occas. Notes R. Astron. Soc.* **3**, 118.
de Vaucouleurs, G., and de Vaucouleurs, A. (1964). 'Reference Catalogue of Bright Galaxies' (Univ. Texas Press).
Whiteoak, J. B., and Gardner, F. F. (1973). *Astrophys. Lett.* **15**, 211.
Whiteoak, J. B., and Gardner, F. F. (1976). *Proc. Astron. Soc. Aust.* **3**, 71.

Manuscript received 27 August 1976